

Cite this: *Chem. Sci.*, 2012, **3**, 3058

www.rsc.org/chemicalscience

EDGE ARTICLE

# Cobalt analogs of Ru-based water oxidation catalysts: overcoming thermodynamic instability and kinetic lability to achieve electrocatalytic O<sub>2</sub> evolution†

Matthew L. Rigsby,<sup>a</sup> Sukanta Mandal,<sup>bc</sup> Wonwoo Nam,<sup>b</sup> Lara C. Spencer,<sup>a</sup> Antoni Llobet<sup>\*bc</sup> and Shannon S. Stahl<sup>\*a</sup>

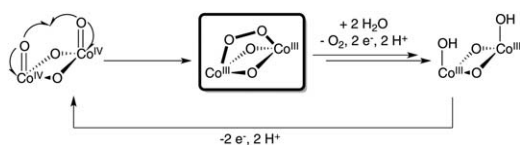
Received 14th June 2012, Accepted 16th July 2012

DOI: 10.1039/c2sc20755a

Several binuclear cobalt(III) complexes that mimic Ru-based water oxidation catalysts have been prepared. The initial complexes exhibited thermodynamic instability and kinetic lability that complicated efforts to use these cobalt complexes as electrocatalysts for water oxidation. Binuclear cobalt(III) complexes supported by a bridging bispyridylpyrazolate (bpp) ligand overcome these limitations. Two bpp-ligated dicobalt(III)-peroxo complexes were prepared and structurally characterized, and electrochemical investigation of these complexes supports their ability to serve as molecular electrocatalysts for water oxidation under acidic conditions (pH 2.1).

## Introduction

Heterogeneous cobalt-oxide materials (CoO<sub>x</sub>) have been the focus of extensive historical,<sup>1</sup> as well as recent,<sup>2</sup> interest as electrochemical water oxidation catalysts (WOCs). This work has provided considerable insight into the electrochemical properties and structural features of these catalysts; however, many questions remain concerning key steps in the catalytic mechanism. Development of well-defined molecular cobalt complexes could facilitate systematic investigation of fundamental steps in Co-mediated water oxidation.<sup>3</sup> A recent computational study of CoO<sub>x</sub> catalysts has implicated Co<sup>III</sup>Co<sup>III</sup>-bridging peroxo intermediates in the water oxidation mechanism (Scheme 1).<sup>4</sup> This



**Scheme 1** Proposed pathway for O–O bond formation in CoO<sub>x</sub>-mediated water oxidation derived from DFT calculations.<sup>4</sup>

<sup>a</sup>Department of Chemistry, University of Wisconsin-Madison, 1101 University Avenue, Madison, Wisconsin 53706, USA. E-mail: stahl@chem.wisc.edu; Fax: +1-608-262-6143; Tel: +1-608-265-6288

<sup>b</sup>Department of Bioinspired Science, Ewha Womans University, 120-750 Seoul, Korea

<sup>c</sup>Institute of Chemical Research of Catalonia (ICIQ), Avinguda Països Catalans 16, E-43007 Tarragona, Spain. E-mail: allobet@icq.es

† Electronic supplementary information (ESI) available: Experimental procedures, compound characterization data. CCDC 885442 and 885443. For ESI and crystallographic data in CIF or other electronic format see DOI: 10.1039/c2sc20755a

work supported our own speculation that peroxo-bridged binuclear Co<sup>III</sup> complexes could serve as entries to well-defined Co WOCs. Here, we describe the investigation of several complexes of this type, including the identification of a kinetically stable binuclear Co complex that mediates electrochemical water oxidation.

Many structural similarities exist between Co and Ru coordination compounds, and the numerous examples of Ru WOCs<sup>5</sup> provided inspiration for structures of possible Co WOCs. Our initial attention focused on the previously reported peroxo-bridged binuclear Co<sup>III</sup> complexes **1** (ref. 6) and **2** (ref. 7) (Chart 1), which are noteworthy for their structural similarity to Ru WOCs. Specifically, the (bpy)(tpy)Co<sup>III</sup> fragments of complex **1** resemble the mononuclear Ru WOCs reported by

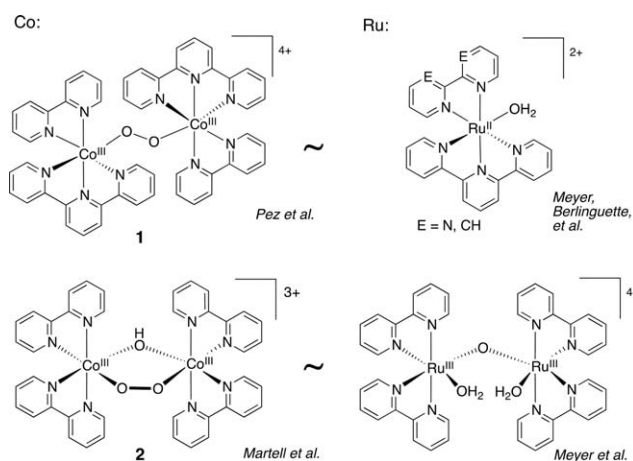


**Chart 1** Structural analogy between Ru-based WOCs and Co-O<sub>2</sub> adducts.

Meyer *et al.*<sup>8</sup> and Berlinguette *et al.*,<sup>9</sup> while the hydroxide-bridged Co<sup>III</sup> complex **2** is reminiscent of Meyer's Ru "blue dimer" WOC.<sup>10</sup>

Aqueous electrochemical studies of complexes **1** and **2**, described below, highlight the kinetic lability of Co–polypyridyl complexes and their tendency to decompose into coordinatively saturated Co–polypyridyl complexes and/or solvated Co ions. This problem was overcome by using a kinetically inert bispyridylpyrazolate (bpp) bridging ligand to stabilize binuclear Co structures, and two bpp-ligated Co<sup>III</sup>Co<sup>III</sup>-( $\mu$ -peroxo) complexes are described herein. Electrochemical studies suggest that these complexes are capable of serving as molecular electrocatalysts for water oxidation. The latter experiments are carried out at pH 2.1, conditions under which heterogeneous and nanoparticulate CoO<sub>x</sub> is not stable, and control experiments provide evidence that the electrocatalytic activity does not arise from free Co ions.

## Results and discussion

### Electrochemical investigation of **1** and **2**

We initiated our studies by investigating the electrochemical properties of previously reported Co-bridging peroxo structures. We chose to examine these complexes in acidic phosphate electrolyte (pH 2.1), reasoning that acidic conditions should stabilize the organic ligands against oxidative decomposition.<sup>11</sup> Furthermore, acidic conditions avoid complications associated with formation of catalytically active, heterogeneous cobalt oxide films or nanoparticles because such materials are unstable with respect to hydrolysis below pH 3–4.<sup>2f</sup>

The peroxo-bridged Co<sup>III</sup> dimer,  $[(\text{tpy})(\text{bpy})\text{Co}^{\text{III}}]_2(\mu\text{-O}_2)](\text{PF}_6)_4$  (**1**), was prepared according to the literature procedure,<sup>6</sup> and a cyclic voltammogram (CV) was recorded in 0.1 M aqueous phosphate electrolyte at pH 2.1. The CV shows a reversible feature at 1.22 V (all potentials referenced to NHE), but no catalytic wave distinct from the background was observed at potentials as high as 2 V (Fig. 1). CVs acquired over the course of several hours revealed a decay of the reversible feature, accompanied by the emergence of a catalytic wave and a new reversible feature at lower potential (0.17 V). The latter feature matches the redox potentials of Co(tpy)<sub>2</sub><sup>2/3+</sup>, analyzed independently under similar conditions (Fig. S1†). On the basis of these observations, the onset of catalytic activity is attributed to free Co ions formed in the decomposition of **1**.<sup>12</sup>

Electrochemical analysis of the hydroxo-bridged Co<sup>III</sup>-peroxo complex **2** initially appeared more promising. A CV of **2** in 0.1 M

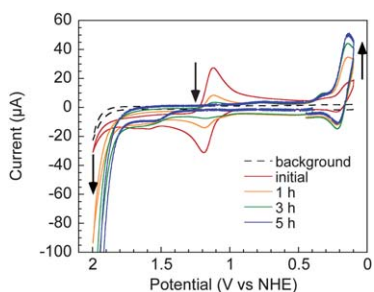


**Fig. 1** CVs of  $[(\text{tpy})(\text{bpy})\text{Co}^{\text{III}}]_2(\mu\text{-O}_2)](\text{PF}_6)_4$  (**1**) (0.25 mM) in 0.1 M pH 2.1 phosphate.

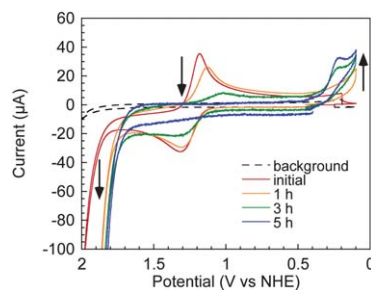
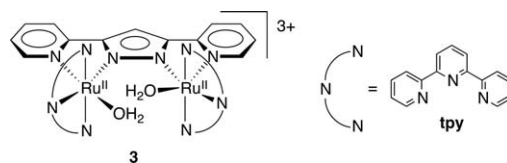


**Fig. 2** CVs of the hydroxo-peroxo-bridged  $(\text{bpy})_2\text{Co}^{\text{III}}$  dimer **2** (0.25 mM) in 0.1 M pH 2.1 phosphate.

pH 2.1 phosphate exhibits a reversible redox feature at 1.25 V together with an apparent catalytic wave at approximately 1.9 V (Fig. 2). Further studies, however, revealed that this complex decomposes under the reaction conditions. The UV-visible spectrum of **2** bleaches, even in the absence of an applied potential (Fig. S4†), and CVs acquired from this solution (Fig. 2) exhibit a decrease in the reversible redox feature, together with a shift of the catalytic wave to lower potential and concomitant growth of an irreversible reductive feature matching that of Co(bpy)<sub>3</sub><sup>3+</sup> (Fig. S5†). These observations demonstrate that **2** is not stable under acidic aqueous conditions and decomposes to Co(bpy)<sub>3</sub> and free Co ions in solution.

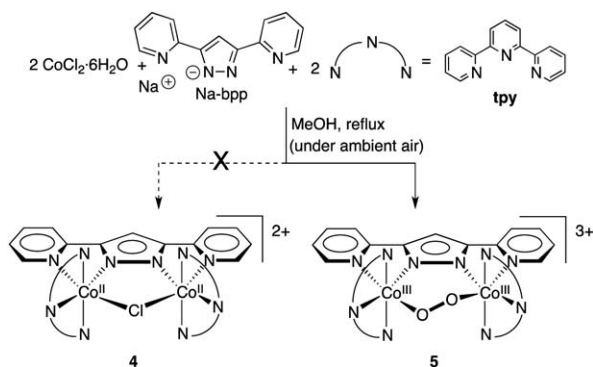
### Bispyridylpyrazolate: a kinetically stable ligand framework

The results obtained with complexes **1** and **2** draw attention to the kinetic lability and thermodynamic instability of molecular Co complexes in aqueous media. Previously reported mononuclear Co WOCs feature rigid, non-labile ancillary ligands, including a corrole<sup>3a</sup> and a pentadentate polypyridyl<sup>3b,c</sup> ligand. These considerations prompted us to consider whether use of bispyridylpyrazolate (bpp) as a bridging ligand could stabilize a binuclear Co complex with respect to hydrolysis, ligand exchange and/or oxidative degradation. This ligand extends the Ru/Co analogy illustrated in Scheme 1, in light of extensive previous studies of a bpp-supported Ru WOC (**3**).<sup>13</sup>



Our initial effort to prepare a binuclear Co–bpp complex targeted the chlorido-bridged derivative **4**, which is directly analogous to a previously reported Ru complex (Scheme 2).<sup>13</sup> CoCl<sub>2</sub>·6H<sub>2</sub>O, Na(bpp) and tpy were refluxed in MeOH under ambient air; however, formation of **4** was not observed. Instead, this reaction led to a deep purple solution, from which the dicobalt(III) complex **5**, containing a bridging end-on peroxide ligand, was isolated and characterized by X-ray crystallography (Fig. 3; see ESI† for details).<sup>14</sup>

In contrast to the observations with complexes **1** and **2**, complex **5** is stable in aqueous 0.1 M, pH 2.1 phosphate over a period of several hours with no signs of degradation or decomposition (Fig. S7†). Cyclic voltammetry of **5** reveals a quasi-reversible



Scheme 2 Preparation of  $[\text{Co}(\text{tpy})]_2(\mu\text{-bpp})(\mu\text{-1,2-O}_2)^{3+}$  complex **5**.

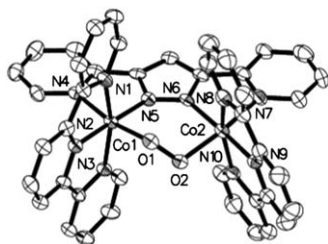


Fig. 3 A molecular diagram of the X-ray structure of **5** shown with 40% probability ellipsoids, all hydrogen atoms and counter ions removed for clarity.

one-electron oxidation ( $E_{\text{mp}} = 1.56$  V) and a catalytic wave at approximately 1.91 V (Fig. 4).<sup>15</sup> Differential pulse voltammetry of **5** using a glassy carbon working electrode<sup>16</sup> reveals the presence of two oxidation waves of approximately equal intensity at 1.56 and 1.82 V. The latter feature corresponds to the onset of the catalytic wave observed by CV. These observations reveal that the  $\text{Co}^{\text{III}}\text{Co}^{\text{III}}$  dimer must be oxidized by two electrons before catalytic turnover is initiated.

In order to characterize the one-electron oxidized species, a solution of **5** in 0.1 M triflic acid was treated with one equivalent of ceric ammonium nitrate.<sup>17</sup> EPR spectroscopy of the one-electron oxidized species reveals a broad signal centered at  $g = 2.01$  (Fig. 5). This signal is consistent with the formation of a low-spin  $S = 1/2$  mixed-valent  $\text{Co}^{\text{III}}\text{Co}^{\text{IV}}$  species.  $\text{Co}^{\text{IV}}$  species have been reported in heterogeneous  $\text{CoO}_x$  WOCs even at potentials

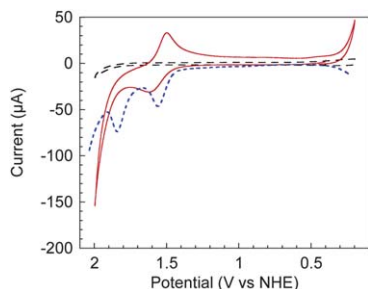


Fig. 4 CVs of FTO background (black dashed), and **5** (0.25 mM) in 0.1 M pH 2.1 phosphate (red solid) and a differential pulse voltammogram of **5** (0.5 mM) using a glassy carbon working electrode (blue dashed), amplitude = 50 mV, pulse period = 0.3 seconds, vertical axis expanded four-fold for clarity.

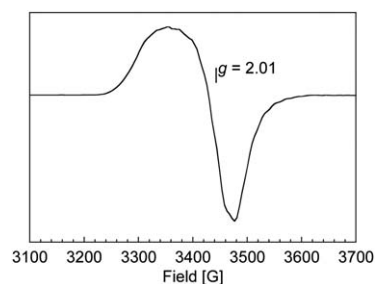


Fig. 5 X-band EPR spectrum of one-electron oxidized **5** (0.5 mM) in frozen aqueous pH 1 triflic acid at 5 K.

prior to the onset of catalysis.<sup>2e,f</sup> The  $\text{Co}^{\text{IV}}\text{Co}^{\text{IV}}$  oxidation level is necessary to induce catalytic water oxidation.

In order to confirm that the catalytic wave observed by CV is in fact associated with production of oxygen, controlled potential electrolysis was performed on a stirred aqueous solution of **5** at 2.0 V and oxygen evolution was detected by using a fluorescence-quench probe. During a two-hour electrolysis, catalytic  $\text{O}_2$  evolution was observed with a Faradaic efficiency for  $\text{O}_2$  production of 77% (Fig. S9†). Some, if not all, of the deviation between observed and theoretical  $\text{O}_2$  yield can be attributed to  $\text{O}_2$  bubbles that accumulate on the electrode and walls of the electrolysis cell, which do not contribute to the  $\text{O}_2$  detected in the headspace. GC analysis of the gas headspace reveals only trace quantities of  $\text{CO}_2$ .<sup>18</sup>

### Evidence for molecular catalysis

One intrinsic challenge in the field of molecular water oxidation catalysis is confirming that the complexes retain their molecular nature under the forcing conditions required for catalyst turnover.<sup>19</sup> This issue is particularly challenging because, in many cases, decomposition products exhibit higher catalytic activity than the well-defined molecular species.<sup>20</sup> Heterogeneous and nanoparticulate  $\text{CoO}_x$  is not stable under the acidic conditions studied here<sup>2f</sup> and can be safely excluded as the basis for the observed catalytic activity. Nevertheless, aqueous Co ions can catalyze water oxidation at the high potentials investigated here (see below), and decomposition of the molecular complex with concomitant release of free Co ions could account for the observed catalytic activity.

If the dimeric Co complex **5** is serving as the true catalyst, it should be possible to modulate catalytic activity in a predictable way by changing the ancillary ligand(s). In order to explore this possibility, we prepared an analog of **5** by replacing the tpy ligand with the more electron-donating bis-(*N*-methylimidazolyl)-pyridine ( $\text{Me}_2\text{bimpy}$ ) ligand. Structure determination by X-ray diffraction confirms formation of the corresponding bridging peroxo complex **6** (Fig. 6).

A comparison of the cyclic voltammograms of **5** and **6** reveals that the quasi-reversible and catalytic waves for **6** shift to lower potential ( $E_{\text{mp}} = 1.35$  V and  $E_{\text{cat}} = 1.84$  V (ref. 15)) relative to **5** (Fig. 7). These changes are consistent with the expected trends upon replacing tpy with a more electron-donating ligand.

Controlled-potential electrolysis studies of **5** and **6** at 2.0 V exhibit stable steady-state currents over the course of five hours, and **6** exhibit a higher current than **5** (Fig. 8), as expected from

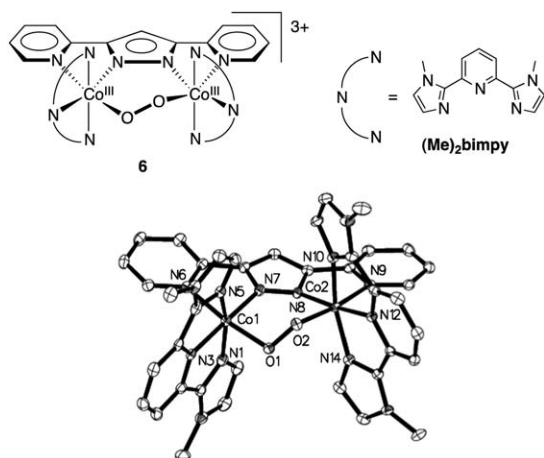


**Fig. 6** A molecular diagram of the X-ray structure of **6** shown with 40% probability ellipsoids, all hydrogen atoms and counter ions removed for clarity.

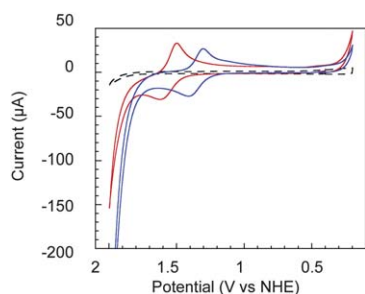


**Fig. 7** CVs of FTO background (black dashed), complex **5** (red), and complex **6** (blue) in 0.1 M pH 2.1 phosphate. [**5** or **6**] = 0.25 mM.

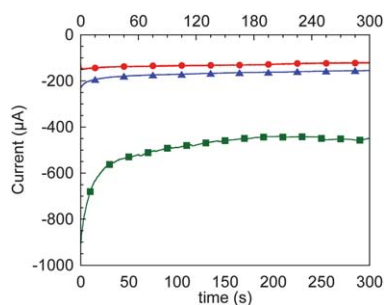
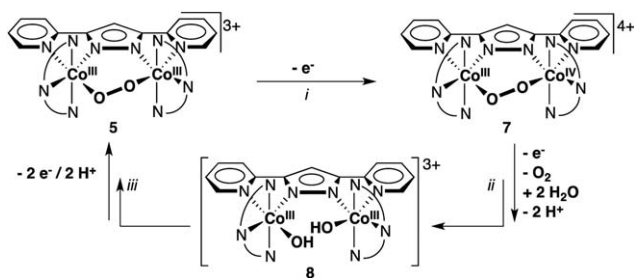


**Fig. 8** Controlled potential electrolysis of complex **5** (red, ● circles), complex **6** (blue, ▲ triangles), and  $\text{CoSO}_4$  (green, ■ squares) at 2.0 V in stirred solution of 0.1 M pH 2.1 phosphate; [analyte] = 0.25 mM.

the CV data. This systematic modulation of the redox potential and steady-state catalytic current upon changing the ancillary ligand environment provides evidence that water oxidation catalysis is mediated directly by molecular species **5** and **6**. However, it is difficult to rigorously exclude the possibility that  $\text{O}_2$  evolution arises from decomposition of **5** and **6**.<sup>21</sup> During electrolysis, however, we do not observe an increase in the catalytic currents, as might be expected if **5** and **6** decompose into free Co ions over the course of prolonged electrolysis.



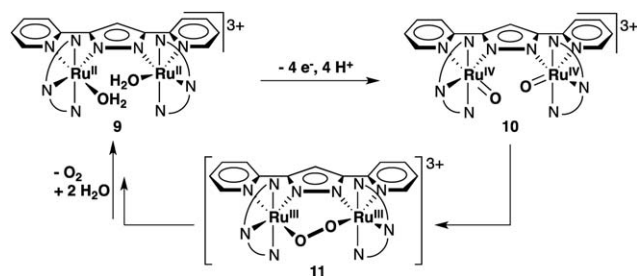
**Scheme 3** Proposed mechanistic framework for water oxidation involving peroxo-bridged  $\text{Co}^{\text{III}}$  dimer **5**.

### Mechanistic discussion and conclusion

The mechanism of water oxidation catalyzed by complexes **5** and **6** is the focus of ongoing investigation. However, the data presented above provide the basis for a preliminary mechanistic framework (Scheme 3). The quasi-reversible redox features evident in the CVs of **5** and **6** (Fig. 4 and 7) are attributed to one-electron oxidation of the dicobalt(III) complex to afford a peroxo-bridged  $\text{Co}^{\text{III}}\text{Co}^{\text{IV}}$  species **7** (Scheme 3, step i). The DPV data suggest that the  $\text{Co}^{\text{III}}\text{Co}^{\text{IV}}$  species **7** undergoes further one-electron oxidation prior to the release of  $\text{O}_2$ . Hydrolysis of the intermediate  $\text{Co}^{\text{IV}}\text{Co}^{\text{IV}}$ -peroxo species (with proton transfers) would release  $\text{O}_2$  and generate a  $\text{Co}^{\text{III}}\text{Co}^{\text{III}}$  dihydroxo species **8**. A two-electron oxidation of **8** with concomitant proton transfers (either in a stepwise or concerted fashion) would close the catalytic cycle (Scheme 3, step iii).

Though heterogeneous water oxidation by  $\text{CoO}_x$  films or nanoparticles is not operative under the pH conditions investigated here, the water oxidation pathway outlined in Scheme 3 closely resembles the fundamental molecular steps proposed mechanism for water oxidation by heterogeneous  $\text{CoO}_x$  electrocatalysts. In  $\text{CoO}_x$  catalyst films, octahedral cobalt centers have been shown to undergo progressive oxidation from  $\text{Co}^{\text{III}}$  to  $\text{Co}^{\text{IV}}$  prior to water oxidation. Water oxidation activity is associated with oxidation of the catalyst to the  $\text{Co}^{\text{IV}}\text{Co}^{\text{IV}}$  oxidation level.<sup>2e,f</sup> Complex **5** mimics this feature, and is the first direct observation of a  $\text{Co}^{\text{IV}}$  intermediate in a molecular WOC.<sup>22</sup>

The dimeric hydroxo- $\text{Co}^{\text{III}}$  intermediate **8** and its conversion into the peroxo-bridged dicobalt(III) species **5** are not directly observed; however, a closely related transformation has been observed with the analogous  $\text{bpp-Ru}$  WOC (Scheme 4).<sup>13</sup> The aqua- $\text{Ru}^{\text{II}}$  dimer **9** has been isolated, and it undergoes a series of proton-coupled electron-transfer steps to afford the dioxo- $\text{Ru}^{\text{IV}}\text{Ru}^{\text{IV}}$  complex **10**. Oxygen evolution proceeds spontaneously from **10**. The peroxo-bridged  $\text{Ru}^{\text{III}}\text{Ru}^{\text{III}}$  intermediate **11** is



**Scheme 4** Mechanism of water oxidation by  $\text{Ru}(\text{bpp})$  WOC.

not observed, but its involvement is supported by  $^{18}\text{O}$  isotopic labeling studies and DFT calculations. On the basis of this precedent, we propose that the hydroxo-Co<sup>III</sup> dimer **8** undergoes two proton-coupled electron-transfer steps to afford a dioxo-Co<sup>IV</sup>Co<sup>IV</sup> intermediate, followed by O–O bond-formation to generate the peroxo-bridged Co<sup>III</sup>Co<sup>III</sup> species **5**. Thus, the molecular bpp-ligated Co and Ru complexes appear to mediate water oxidation by qualitatively similar mechanisms, but they exhibit differences in the relative energies of intermediates and the precise sequence of individual reaction steps (e.g., proton/electron transfers). Future experimental and computational studies should allow us to acquire important additional insights into the mechanistic relationship between Co and Ru WOCs.

In summary, we have prepared a series of Co<sup>III</sup>Co<sup>III</sup> bridging-peroxo complexes that bear structural resemblance to previously studied Ru WOCs. These studies highlight the importance of a non-labile ligand framework to minimize ligand exchange and decomposition of the Co complex under the forcing conditions required to achieve water oxidation. Use of the bridging anionic chelating bpp ligand achieves this goal and provides the basis for the observation and systematic investigation of catalytic water oxidation by a well-defined binuclear Co complex.

## Acknowledgements

The authors thank James Gerken for many helpful conversations. This research was supported by the NSF under CCI Powering the Planet grant CHE-0802907 (S.S.S.), and by MICINN CTQ2010-21497 Spain (A.L.) and the WCU Program (R31-100100) Korea (W.N., A.L.).

## Notes and references

- For leading references, see: (a) J. O'M. Bockris and T. Otagawa, *J. Phys. Chem.*, 1983, **87**, 2960; (b) J. O'M. Bockris and T. Otagawa, *J. Electrochem. Soc.*, 1984, **131**, 290; (c) Y.-W. D. Chen and R. N. Noufi, *J. Electrochem. Soc.*, 1984, **131**, 1447.
- See, for example: (a) M. W. Kanan and D. G. Nocera, *Science*, 2008, **321**, 1072; (b) Y. Surendranath, M. Dincă and D. G. Nocera, *J. Am. Chem. Soc.*, 2009, **131**, 2615; (c) Y. Surendranath, M. W. Kanan and D. G. Nocera, *J. Am. Chem. Soc.*, 2010, **132**, 16501; (d) M. Risch, V. Khare, I. Zaharieva, L. Gerencser, P. Chernev and H. Dau, *J. Am. Chem. Soc.*, 2009, **131**, 6936; (e) J. G. McAlpin, Y. Surendranath, M. Dincă, T. A. Stich, S. A. Stoian, W. H. Casey, D. G. Nocera and R. D. Britt, *J. Am. Chem. Soc.*, 2010, **132**, 6882; (f) J. B. Gerken, J. G. McAlpin, J. Y. Chen, M. L. Rigsby, W. H. Casey, R. D. Britt and S. S. Stahl, *J. Am. Chem. Soc.*, 2011, **133**, 14431; (g) F. Jiao and H. Frei, *Angew. Chem., Int. Ed.*, 2009, **48**, 1841; (h) A. J. Esswein, M. J. McMurdo, P. N. Ross, A. T. Bell and T. D. Tilley, *J. Phys. Chem. C*, 2009, **113**, 15068.
- Two mononuclear Co WOCs have been reported recently: (a) D. K. Dogutan, R. McGuire and D. G. Nocera, *J. Am. Chem. Soc.*, 2011, **133**, 9178; (b) D. J. Wasylenko, C. Ganesamoorthy, J. Borau-Garcia and C. P. Berlinguette, *Chem. Commun.*, 2011, **47**, 4249; (c) D. J. Wasylenko, R. D. Palmer, E. Schott and C. P. Berlinguette, *Chem. Commun.*, 2012, **48**, 2107; (d) For an example of an all-inorganic cobalt-based molecular water oxidation catalyst, see: Q. Yin, J. M. Tan, C. Besson, Y. V. Geletii, D. G. Musaev, A. E. Kuznetsov, Z. Luo, K. I. Hardcastle and C. L. Hill, *Science*, 2010, **328**, 342.
- L.-P. Wang and T. Van Voorhis, *J. Phys. Chem. Lett.*, 2011, **2**, 2200.
- X. Sala, I. Romero, M. Rodríguez, L. Escriche and A. Llobet, *Angew. Chem., Int. Ed.*, 2009, **48**, 2842.
- D. Ramprasad, A. G. Gilcinski, T. J. Markley and G. P. Pez, *Inorg. Chem.*, 1994, **33**, 2841.
- R. F. Bogucki, G. McLendon and A. E. Martell, *J. Am. Chem. Soc.*, 1976, **98**, 3202.
- (a) J. J. Concepcion, J. W. Jurss, J. L. Templeton and T. J. Meyer, *J. Am. Chem. Soc.*, 2008, **130**, 16462; (b) J. J. Concepcion, M.-K. Tsai, J. T. Muckerman and T. J. Meyer, *J. Am. Chem. Soc.*, 2010, **132**, 1545.
- D. J. Wasylenko, C. Ganesamoorthy, M. A. Henderson, B. D. Koivisto, H. D. Osthoff and C. P. Berlinguette, *J. Am. Chem. Soc.*, 2010, **132**, 16094.
- (a) S. W. Gersten, G. J. Samuels and T. J. Meyer, *J. Am. Chem. Soc.*, 1982, **104**, 4029; (b) J. A. Gilbert, D. S. Eggleston, W. R. Murphy, D. A. Geselowitz, S. W. Gersten, D. J. Hodgson and T. J. Meyer, *J. Am. Chem. Soc.*, 1985, **107**, 3855; (c) R. A. Binstead, C. W. Chronister, J. Ni, C. M. Hartshorn and T. J. Meyer, *J. Am. Chem. Soc.*, 2000, **122**, 8464.
- Ru polypyridyl complexes have been shown to undergo more facile ligand oxidation at higher pH. For leading references, see: (a) L. Roecker, W. Kutner, J. A. Gilbert, M. Simmons, R. W. Murray and T. J. Meyer, *Inorg. Chem.*, 1985, **24**, 3784; (b) J. K. Hurst, *Coord. Chem. Rev.*, 2005, **249**, 313.
- Electrochemical studies performed at higher pH (e.g., 0.1 M phosphate, pH 7) led to formation of a catalytically active heterogeneous deposit on the electrode (see ESI†). Acidic conditions were chosen for the remainder of these studies because CoOx is thermodynamically unstable under these conditions.
- (a) C. Sens, I. Romero, M. Rodríguez, A. Llobet, T. Parella and J. Benet-Buchholz, *J. Am. Chem. Soc.*, 2004, **126**, 7798; (b) F. Bozoglian, S. Romain, M. Z. Ertem, T. K. Todorova, C. Sens, J. Mola, M. Rodríguez, I. Romero, J. Benet-Buchholz, X. Fontrodona, C. J. Cramer, L. Gagliardi and A. Llobet, *J. Am. Chem. Soc.*, 2009, **131**, 15176.
- Complex **5** was discovered independently in the labs of Stahl and Llobet/Fukuzumi/Nam. For the investigation of **5** in catalytic, four-electron reduction of O<sub>2</sub>, see: S. Fukuzumi, S. Mandal, K. Mase, K. Ohkubo, H. Park, J. Benet-Buchholz, W. Nam and A. Llobet, *J. Am. Chem. Soc.*, 2012, **134**, 9906.
- Catalytic onset is defined here as the potential in an anodic scan at which the current is two fold higher than the quasi-reversible anodic peak current.
- Attempts to record DPVs with FTO electrodes display a single, broad feature in which the two redox processes are not well-resolved. This behavior is attributed to the slower heterogeneous electron transfer rate with FTO versus glassy carbon.
- Ceric ammonium nitrate is not a strong enough oxidant to promote catalytic water oxidation by **5**; however, it is capable of oxidizing **5** by one electron to **7**. See Fig. S11† for CV/DPV data in 0.1 M triflic acid.
- Gas chromatographic analysis (TCD detector) of the headspace gas revealed the formation of 1.8 μmoles of CO<sub>2</sub>, which would account for ~3% of the current passed during electrolysis. Under identical conditions, 26 μmoles of O<sub>2</sub> are detected.
- R. H. Crabtree, *Chem. Rev.*, 2012, **112**, 1536.
- For recent discussion of decomposition of proposed molecular water oxidation catalysts to catalytically-active products, see: (a) J. J. Stracke and R. G. Finke, *J. Am. Chem. Soc.*, 2011, **133**, 14872; (b) D. Hong, J. Jung, J. Park, Y. Yamada, T. Suenobu, Y.-M. Lee, W. Nam and S. Fukuzumi, *Energy Environ. Sci.*, 2012, **5**, 7606; (c) N. D. Schley, J. D. Blakemore, N. K. Subbaiyan, C. D. Incarvito, F. D'Souza, R. H. Crabtree and G. W. Brudvig, *J. Am. Chem. Soc.*, 2011, **133**, 10473; (d) D. B. Grotjahn, D. B. Brown, J. K. Martin, D. C. Marelius, M.-C. Abadjian, H. N. Tran, G. Kalyuzhny, K. S. Vecchio, Z. G. Specht, S. A. Cortes-Llamas, V. Miranda-Soto, C. van Niekerk, C. E. Moore and A. L. Rheingold, *J. Am. Chem. Soc.*, 2011, **133**, 19024.
- The stability of the Co complexes **5** and **6** during electrolysis were analysed by UV-visible spectroscopy and CV. Although some decay of the complexes is evident, this decay does not correlate with enhanced catalytic activity. See ESI† for data and additional commentary.
- For EPR characterization of Co<sup>IV</sup> in a catalytically-inactive oxo-bridged cobalt cubane complex, see: J. G. McAlpin, T. A. Stich, C. A. Ohlin, Y. Surendranath, D. G. Nocera, W. H. Casey and R. D. Britt, *J. Am. Chem. Soc.*, 2011, **133**, 15444.